JOURNAL OF GUIDANCE, CONTROL, AND DYNAMICS
Vol. 20, No. 5, September–October 1997

Two-Dimensional Active Wing/Store Flutter Suppression Using $\mathcal{H}_\infty$ Theory

Prasad V. N. Gade* and Daniel J. Inman†
Virginia Polytechnic Institute and State University, Blacksburg, Virginia 24061

An active method of decoupling the wing from store pitch inertia effects is presented for the wing/store flutter suppression problem. The proposed active decoupler pylon involves the use of a piezoceramic wafer strut as an actuator, which acts as a soft spring between the wing and the store. A two-degree-of-freedom typical section of an airfoil is used to represent the structural model of an F-16 aircraft wing, and the flutter problem is studied in incompressible flow regime where the circulatory component of the aero loads is modeled using Jones' approximation to the Theodorsen function. The aerodynamic effects on the store, however, are neglected, and a controller is designed using $\mathcal{H}_\infty$ theory to make the closed-loop system robust to such unstructured uncertainties. Under a set of design specifications quantified as weighting functions, a mixed-sensitivity $\mathcal{H}_\infty$ optimal control synthesis problem is solved for the design of a controller. Singular-value Bode plots of robust stability and nominal performance measures are used for the analysis of the closed-loop system.

Nomenclature

a	= distance between elastic center and midchord
b	= semichord length
g	= structural damping
h	= plunge displacement
i	= $\sqrt{(-1)}$
L_1	= distance between top of strut to elastic center
ℓ	= distance between pivot point to elastic center
m_p	= mass of the piezoceramic wafer actuator
m_s	= mass of the store
m_w	= mass of the wing
r_α	= radius of gyration of airfoil
r_θ	= radius of gyration of pylon/store
s	= Laplace variable
$\bar{s}$	= reduced frequency
U	= freestream velocity
u	= actuator input
x_α	= distance between elastic center and c.g. of wing
x_θ	= distance between c.g. of store to pivot point
x_1, x_2	= aerodynamic lag states
α	= pitch angle of airfoil
γ	= tuning parameter used in weighting functions
Δ	= output multiplicative uncertainty matrix
θ	= pitch angle of store relative to airfoil
$\underline{\sigma}$	= minimum singular value
$\bar{\sigma}$	= maximum singular value
ω_h	= natural frequency of plunging motion
ω_α	= natural frequency of pitching motion of airfoil
ω_θ	= natural frequency of pitching motion of store

Subscripts and Superscript

c	= circulatory components
nc	= noncirculatory components
s	= structural components
~	= transfer function without imaginary axis poles

Introduction

A TOPIC of current interest in the aeronautical community is the flutter suppression of high-performance combat aircraft carrying underwing stores. Fighter aircraft are required to carry several combinations of external stores and perform maneuvers in a variety of flight conditions. The increase in weight due to the addition of store decreases the frequency of the first torsional mode of the wing thereby bringing it closer to the fundamental bending frequency. This coupling between bending and torsional modes results in a substantial decrease in flutter speed. Although passive methods such as structural and mass balance techniques have claimed to alleviate flutter, the associated added weights generally result in decreased aircraft performance. Moreover, the requirement on the aircraft to carry several combinations of stores makes its implementation practically impossible. Although active control technology also has weight penalties due to actuator mass and electronic hardware, the flexibility it offers in addressing robustness issues via modern dynamic feedback controllers places it at an advantageous position relative to passive methods.

This paper uses one such modern robust control methodology, namely, $\mathcal{H}_\infty$ theory, to investigate the robust stability and nominal performance issues associated with aero and structural dynamics uncertainties of a two-dimensional wing/store flutter suppression model. Although store flutter problem is most critical around transonic speeds, this paper analyses it in incompressible flow regime to lay basic foundation for more advanced work in this field. Singular-value plots of robust stability and performance measures as a function of frequency are used for the analysis.

Background and Motivation

Flutter can be alleviated by conventional passive schemes or by the more advanced active approaches. Passive methods typically include adding mass ballast, relocating store location spanwise and/or chordwise, or tuning the pylon stiffness characteristics.[1–3] However, these methods are generally tailored to a specific configuration and fail to accommodate different store mass and location combinations.

Active methods, on the other hand, are relatively more flexible and require mere change of control law to accommodate different store combinations. One of the earliest known works on the feasibility of using active control for wing/store flutter suppression was reported by Triplett[4] in 1972. His analytical study of an F-4 Phantom aircraft wing/store configuration involved deflecting ailerons in a manner to produce aerodynamic forces that opposed the flutter causing aerodynamic forces. A number of investigators have made important contributions to the field of active wing/store flutter suppression.[5,6] In 1979 Harvey et al.[7] investigated the feasibility of using adaptive control for wing/store flutter suppression with this approach. Some researchers proposed a slightly modified version, which involved feeding back signals from the accelerometers at the fore and aft end of the store to electrohydraulic actuators to drive vanes attached to the forward part of the store.[8,9] The deflected vanes generated

Received Nov. 21, 1996; revision received April 14, 1997; accepted for publication April 18, 1997.

*Graduate Research Assistant, Department of Engineering Science and Mechanics. Student Member AIAA.

†Herrick Endowed Professor, Department of Engineering Science and Mechanics. Associate Fellow AIAA.

counteracting aerodynamic forces that stabilized the store pitch motion. Hönlinger and Destuynder[10] used linear quadratic regulator control law to test the procedure on a Phantom F-4F wing/store configuration. However, the effectiveness of these methods depended largely on the accurate knowledge of counteracting unsteady aerodynamic forces produced by the control surfaces. This poses a particular problem especially in the transonic range where the theoretical predictions of the unsteady aerodynamic coefficients of the control surfaces are least reliable.[11]

Triplett's feasibility study[4] in 1972 gained interest in the aeronautical community and was soon followed by an Air Force contract to evaluate the ability of a single wing/store flutter control scheme that would be robust to several different store configurations.[12] Instead of using control surface's unsteady aerodynamics as in the earlier active methods, Triplett et al.[12] proposed to use a hydraulic actuator to decouple the store vibratory motion from that of the wing. Although the dynamic behavior of this scheme worked quite well in restoring bare wing flutter speed, the actuator's inability to meet high-flow-rate requirements for the control of higher frequency perturbations restricted its practical implementation.

In 1980, Reed et al.[11] proposed a modified version of the approach just described. Instead of using a hydraulic actuator as a load carrying tie, a passive soft-spring/damper combination was used together with a low-power active control system to maintain store alignment. Their idea is based on the argument that instead of modifying the aerodynamic forces, the frequencies associated with flutter critical bending and torsion modes can be separated by making the wing insensitive to store pitch inertia and eventually alleviate the adverse coupling to a higher flutter speed. Some researchers[13–17] analytically analyzed this concept and successfully demonstrated its use in wing/store flutter suppression.

The design of the decoupler pylon mounted store consists of pitch-pivot mechanism near the fore end that allows the store to pitch relative to the wing surface. Near the aft end, a soft spring is used to decouple the influence of store pitch inertia on wing torsion modes. A low-frequency feedback control is used to prevent large static deflections and maintain alignment. The result is a substantial increase in flutter speed, well beyond that of the bare wing. Based on a feasibility study,[18] a decoupler pylon was fabricated by Clayton et al.[19] and was later successfully implemented on an F-16 aircraft to increase the flutter speed.

Instead of passive soft-spring/damper elements as used by Reed et al.[11] to demonstrate their concept, the current approach proposes an active decoupler pylon for the control of wing/store flutter suppression. The proposed active isolation scheme, shown in Fig. 1, serves two purposes. First, it decouples the wing dynamics from the store pitch inertia effects, a primary source for bending-torsion flutter in wing with external stores. Second, with the aid of a robust controller, it acts as an actuator that stabilizes and maintains the performance characteristics of the closed-loop system in the face of uncertainties at flutter speed. The active pylon consists of a strut with series of thin circular plates laminated on opposite faces with piezoceramics. The poled directions of the piezoceramics are aligned so that a voltage (control input) applied across the element contracts on one side and expands on the other. The plate bending is then translated into an axial motion along the strut. The piezostrut is designed such that its equivalent stiffness satisfies the Reed et al. criterion[11] of a soft spring system for isolation purposes, i.e., the store pitch to wing bending frequency ratio should always be less than 1 for effective store flutter alleviation. The novelty in this approach is the use of the strut as both a passive isolator as well as an active actuator to maintain stability and performance. The current active concept has two major advantages over other passive schemes.[11,18,19] Not only does the active decoupler make the system more robust to various uncertainties, but it also has significant weight benefits because it gets away with all the hardware that is required with pneumatic springs and hydraulic dashpots. Moreover, compared to that of a hydraulic actuator, the wafer actuator's faster time response to input command signals makes it suitable for store flutter suppression problem.

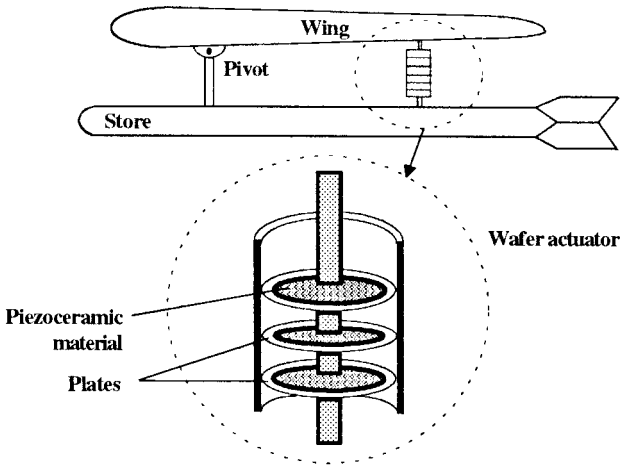

Fig. 1 Wing/store piezostrut arrangement.

It is proposed that this device will represent a significant improvement in the much needed stroke length requirement over the traditional stack actuator proposed by Gade and Flowers.[20] Their results on a wing/store model showed that piezo motors fail in providing the much needed stroke length for restoring the bare wing flutter speed. Moreover, these actuators typically fail in tension because of the brittle nature of the piezoceramic materials. On the other hand, the current bender-element type actuator, initially fabricated and designed[21] for use in a large flexible structure, behaves the same both in tension as well in compression. Several issues pertaining to the actuator are yet to be quantified, such as actuator dynamics, its time response to input command signals relative to hydraulic actuators, stroke length capability over traditional stack actuators, and power requirements. At the time of writing, the dynamics of the actuator has not been identified and, hence, are not included.

In this paper, a controller for wing/store flutter suppression model of an F-16 aircraft with a GBU-8/B store configuration is designed using $\mathcal{H}_\infty$ theory. The wing is modeled using a two-dimensional approximation of a typical section of an airfoil, and the store flutter problem is studied in the incompressible flow regime. The objective is to design a closed-loop control system that is robust to various uncertainties, such as store aerodynamics and other flexible structural modes not taken into account in the model. Singular-value analysis is used to assess the system's nominal performance and robust stability characteristics, in the face of such uncertainties.

Plant Description

The analytical model is restricted to a typical section of a thin airfoil with an underwing store in two-dimensional incompressible flow. A sketch of the typical section together with the decoupler pylon and the store is shown in Fig. 2. The plunging or bending motion of the entire airfoil/store combination together with pitch angles of the lifting surface, α, and the store, θ, measured relative to the undeformed wing constitute the three degrees of freedom of wing/store model. Linear and torsional springs at the elastic center

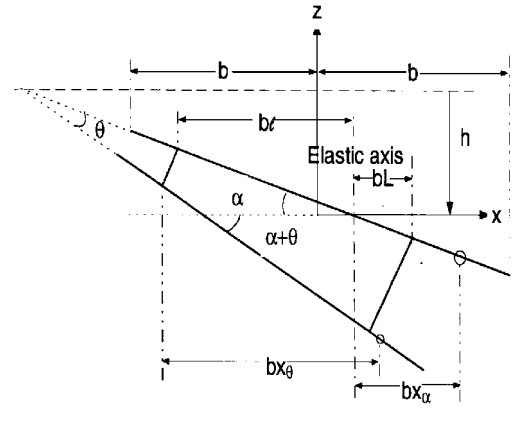

Fig. 2 Schematic diagram of a thin airfoil and decoupler-pylon-mounted store.

are used to model the restraining forces to the vertical and angular displacements of the airfoil, whereas restraint to the pitching motion of the store is provided by the decoupler pylon mechanism. Standard sign convention is used in which the plunging displacement is measured positive downward, whereas a nose-up position of the structure implies a positive pitching angle. The total lift on the airfoil is defined positive up whereas the pitching moment of the entire airfoil about the one-quarter chord length point is positive in the nose-up sense. Assuming no structural damping g, the equations of motion in the Laplace domain is given by

$$\boldsymbol{M}_s\ddot{\boldsymbol{z}} + \boldsymbol{K}_s\boldsymbol{z} = \begin{Bmatrix} -L \\ M \\ 0 \end{Bmatrix} + \begin{Bmatrix} Q_h \\ Q_\alpha \\ Q_\theta \end{Bmatrix} \tag{1}$$

where

$$\boldsymbol{z}(\boldsymbol{t}) = \{h/b \quad \alpha \quad \theta\}^T$$

is a vector of generalized coordinates in which the plunge motion h of the airfoil is nondimensionalized by its semichord length b to enable easy comparison with the pitching motions. The left-hand side of Eq. (1) consists of the mass and elastic terms of the airfoil, the actuator, and the attached store and is given as

$$\boldsymbol{M}_s = \begin{bmatrix} m_w + m_s + m_p & m_w x_\alpha + m_p L_1 + m_s(x_\theta - \ell) & m_s x_\theta + \frac{1}{2} m_p L_1 \\ m_w x_\alpha + m_p L_1 + m_s(x_\theta - \ell) & m_w r_\alpha^2 + m_p L_1^2 + m_s\left(r_\theta^2 + \ell^2 - 2x_\theta \ell\right) & m_s\left(r_\theta^2 - x_\theta \ell\right) + \frac{1}{2} m_p L_1^2 \\ m_s x_\theta + \frac{1}{2} m_p L_1 & m_s\left(r_\theta^2 - x_\theta \ell\right) + \frac{1}{2} m_p L_1^2 & m_s r_\theta^2 + \frac{1}{3} m_p L_1^2 \end{bmatrix}$$

$$\boldsymbol{K}_s = \begin{bmatrix} m_w \omega_h^2 & 0 & 0 \\ 0 & m_w r_\alpha^2 \omega_\alpha^2 & 0 \\ 0 & 0 & m_s r_\theta^2 \omega_\theta^2 \end{bmatrix} \tag{2}$$

The terms on the right-hand side of Eq. (1) correspond to the aerodynamics identified as the lift L and the moment M. A method for calculating the aerodynamic loads due to simple harmonic oscillations of a wing section in incompressible flow was first given by Theodorsen.[22] The theory was then extended to arbitrary motions by Edwards.[23] His generalized unsteady aerodynamic theory divides the aerodynamic loads into noncirculatory and circulatory parts and are expressed in the Laplace domain as

$$\begin{Bmatrix} -L \\ M \\ 0 \end{Bmatrix} = \left(-s^2 \boldsymbol{M}_{\mathrm{nc}} - s\boldsymbol{C}_{\mathrm{nc}} + s\boldsymbol{C}_c + \boldsymbol{K}_c\right)\boldsymbol{z}(\boldsymbol{s}) \tag{3}$$

where $\boldsymbol{M}_{\mathrm{nc}}$ and $\boldsymbol{C}_{\mathrm{nc}}$ are apparent additional mass and damping matrices due to noncirculatory oscillations of the aerodynamic loads given by

$$\boldsymbol{M}_{\mathrm{nc}} = \begin{bmatrix} 1 & -a & 0 \\ -a & a^2 + \frac{1}{8} & 0 \\ 0 & 0 & 0 \end{bmatrix} \qquad \boldsymbol{C}_{\mathrm{nc}} = \frac{U}{b}\begin{bmatrix} 0 & 1 & 0 \\ 0 & \frac{1}{8} - a & 0 \\ 0 & 0 & 0 \end{bmatrix} \tag{4}$$

whereas $\boldsymbol{C}_c$ and $\boldsymbol{K}_c$ matrices correspond to the circulatory part, which are further subdivided into

$$s\boldsymbol{C}_c + \boldsymbol{K}_c = C(\bar{s})\boldsymbol{R}[s\boldsymbol{S}_2 + \boldsymbol{S}_1] \tag{5}$$

where

$$\boldsymbol{R} = \begin{Bmatrix} -2 \\ 2\left(a + \frac{1}{2}\right) \\ 0 \end{Bmatrix} \qquad \boldsymbol{S}_1 = [0 \quad 1 \quad 0] \qquad \boldsymbol{S}_2 = \begin{bmatrix} 1 & \frac{1}{2} - a & 0 \end{bmatrix}$$

In Eq. (5), $C(\bar{s})$ represents the complex Theodorsen function, where $\bar{s} = b\omega i/U$ is a Laplace operator associated with nondimensional time Ut/b. The effects of aerodynamics on the store, however, are neglected to make the analysis simpler. With the aid of multivariable robust control techniques, the influence of unmodeled dynamics on the stability and nominal performance of the wing/store flutter suppression system is evaluated in the following. The complete equation of motions is recast into the form

$$\left\{s^2(\boldsymbol{M}_s + \boldsymbol{M}_{\mathrm{nc}}) + s\boldsymbol{C}_{\mathrm{nc}} + \boldsymbol{K}_s\right\}\boldsymbol{z}(\boldsymbol{s}) = C(\bar{s})\boldsymbol{R}[s\boldsymbol{S}_2 + \boldsymbol{S}_1]\boldsymbol{z}(\boldsymbol{s}) + \boldsymbol{H}\boldsymbol{u}(\boldsymbol{s}) \tag{6}$$

where $\boldsymbol{u}$ is the actuator input acting through the input matrix $\boldsymbol{H} = [0 \ 0 \ 1]^T$ due to the generalized actuator forces Q_i given in Eq. (1). To complete the model in the Laplace domain, Jones's[24] second-order rational approximation to the complex Theodorsen function is used and is given by

$$C(\bar{s}) = \frac{0.5(sb/U)^2 + 0.2808(sb/U) + 0.01365}{(sb/U)^2 + 0.3455(sb/U) + 0.01365} \tag{7}$$

A nonunique state-space representation of the Jones' approximation for unsteady circulatory aerodynamic load can be obtained as

$$\left[\begin{array}{c|c} \boldsymbol{A}_2 & \boldsymbol{B}_2 \\ \hline \boldsymbol{C}_2 & \boldsymbol{D}_2 \end{array}\right] = \left[\begin{array}{cc|c} -0.3(U/b) & 0 & -1.2650(U/b) \\ 0 & -0.0455(U/b) & -0.4927(U/b) \\ \hline -0.0799 & -0.0151 & 0.5 \end{array}\right] \tag{8}$$

The state-space representation of the structural equations and noncirculatory components of the aerodynamic loads is given as

$$\left[\begin{array}{c|c} \boldsymbol{A}_1 & \boldsymbol{B}_1 \\ \hline \boldsymbol{C}_1 & \boldsymbol{D}_1 \end{array}\right] = \left[\begin{array}{cc|c} \boldsymbol{0} & \boldsymbol{I} & \boldsymbol{0} \\ -(\boldsymbol{M}_s + \boldsymbol{M}_{\mathrm{nc}})^{-1}\boldsymbol{K}_s & -(\boldsymbol{M}_s + \boldsymbol{M}_{\mathrm{nc}})^{-1}\boldsymbol{C}_{\mathrm{nc}} & (\boldsymbol{M}_s + \boldsymbol{M}_{\mathrm{nc}})^{-1}\boldsymbol{R} \\ \hline (U/b)^2\boldsymbol{S}_1 & (U/b)\boldsymbol{S}_2 & \boldsymbol{0} \end{array}\right] \tag{9}$$

From Eq. (8) it is evident that the circulatory aerodynamic loads introduce two additional states, called the aerodynamic lags (x_1 and x_2), which increase the total number of states to eight. The state-space representation of the augmented system is given by

$$\dot{\boldsymbol{x}} = \boldsymbol{A}\boldsymbol{x} + \boldsymbol{B}\boldsymbol{u} \qquad \boldsymbol{y} = \boldsymbol{C}\boldsymbol{x} + \boldsymbol{D}\boldsymbol{u} \tag{10}$$

where

$$\boldsymbol{x} = \{h/b \quad \alpha \quad \theta \quad \dot{h}/b \quad \dot{\alpha} \quad \dot{\theta} \quad x_1 \quad x_2\}^T$$

and

$$\left[\begin{array}{c|c} \boldsymbol{A} & \boldsymbol{B} \\ \hline \boldsymbol{C} & \boldsymbol{D} \end{array}\right] = \left[\begin{array}{cc|c} \boldsymbol{A}_1 + \boldsymbol{B}_1\boldsymbol{D}_2\boldsymbol{C}_1 & \boldsymbol{B}_1\boldsymbol{C}_2 & (\boldsymbol{M}_s + \boldsymbol{M}_{\mathrm{nc}})^{-1}\boldsymbol{H} \\ \boldsymbol{B}_2\boldsymbol{C}_1 & \boldsymbol{A}_2 & \boldsymbol{0} \\ \hline \boldsymbol{I} & \boldsymbol{0} & \boldsymbol{0} \end{array}\right] \tag{11}$$

The three primary outputs of interest considered here are the plunging motion h, wing pitch α, and the relative store pitch angle θ. The state-space realization [Eq. (11)] is now in a form suitable for applying modern control laws.

Uncertainty Representation

The dynamics of any physical system can never be captured completely by mathematical models. There are always errors associated with the approximations made during the modeling process. These

approximations are made either due to lack of complete knowledge of the system or due to difficulty in modeling. For instance, the plant described in the preceding section does not include actuator dynamics and aero loads on the actuator and the store. During the design of an appropriate controller, the robustness of the closed-loop system in the face of these uncertainties and maintenance of its nominal performance are, therefore, the primary objectives of a control engineer.

In robust control literature, the mathematical representation of uncertainties due to such unintentional exclusion of high-frequency dynamics, generally take many forms,[25] of which the most commonly used is the multiplicative uncertainty model. Depending on where the errors are reflected with respect to the plant, the uncertainty is classified into input or output multiplicative models. If $\Delta(s)$ represents a proper and stable approximation transfer function error, then the nominal plant $[\boldsymbol{G}(s)]$ perturbed with the output multiplicative uncertainty model is given as

$$\boldsymbol{G}^*(s) = [\mathbf{1} + \Delta(s)]\boldsymbol{G}(s) \tag{12}$$

By applying small gain theorem[26] to the loop obtained using $\Delta(s)$, the nominal plant $\boldsymbol{G}(s)$, and the controller $\boldsymbol{K}(s)$ to be discussed later, the size of the multiplicative error $\Delta(j\omega)$ at each frequency can be calculated. This principal gain plot then represents the relative percentage magnitude of the unstructured perturbations that the system will be able to withstand.

Mixed-Sensitivity Objective

In $\mathcal{H}_\infty$ control literature,[27] it is common to first identify the objective functions whose infinity norm is to be minimized. Typically, they are either single- or multitarget objectives involving sensitivity function $\boldsymbol{S}(s)$, complementary sensitivity function $\boldsymbol{T}(s)$, and/or control-input constraint function $\boldsymbol{U}(s)$. $\boldsymbol{S}(s)$ is used for achieving good stability margins whereas $\boldsymbol{T}(s)$ is used for achieving robustness for uncertainty in dynamic modeling.

This paper attempts to investigate the feasibility of designing a $\mathcal{H}_\infty$ controller-based, closed-loop system that is robust to uncertainties due to store aerodynamics and other high-frequency flexible structural modes that have been ignored. The designed closed-loop system is also intended to have good performance characteristics such as disturbance rejection, and insensitiveness to low-frequency parameter variations. Changes in the center of gravity location of store, mass, radius of gyration, etc., are some of the examples of parameter variations that may occur in the wing/store flutter suppression problem.

Mathematically, the objectives are equivalent to minimizing the weighted sensitivity $\boldsymbol{S}(s)$ and complementary sensitivity $\boldsymbol{T}(s)$ transfer matrices. Within the framework of $\mathcal{H}_\infty$ control theory, this implies the minimization of the infinity norm[27]

$$\left\| \begin{bmatrix} \boldsymbol{W}_1\boldsymbol{S} \\ \boldsymbol{W}_2\boldsymbol{T} \end{bmatrix} \right\|_\infty = \left\| \begin{bmatrix} \boldsymbol{W}_1(\boldsymbol{I}+\boldsymbol{G}\boldsymbol{K})^{-1} \\ \boldsymbol{W}_2\boldsymbol{G}\boldsymbol{K}(\boldsymbol{I}+\boldsymbol{G}\boldsymbol{K})^{-1} \end{bmatrix} \right\|_\infty < 1 \tag{13}$$

Here the loop is considered to be broken at the output where all of the uncertainties are assumed to be reflected. Based on given performance requirements, frequency-dependent weighting functions $\boldsymbol{W}_1(s)$ and $\boldsymbol{W}_2(s)$ can be appropriately chosen to give the designer relatively more freedom to achieve the desired objectives. Because it is unnecessary to minimize the effect of a cost function over a frequency range in which its effect is least likely, low- and high-pass filters are generally used as weighting functions. Here the objective is to find an admissible controller $\boldsymbol{K}(s)$, which minimizes the given weighted norm subject to the constraint that the closed-loop system be stable.

$\mathcal{H}\infty$ Control Problem Formulation

In $\mathcal{H}_\infty$ control theory, a closed-loop system is usually represented in the form of a two-port block diagram (as shown in Fig. 3), where the input signal vector $\boldsymbol{w}$ consist of all exogenous inputs comprising disturbances, noises, and model-error outputs Δ; $\boldsymbol{u}$ is the controller output; and $\boldsymbol{y}$ is a vector of input signals consisting of measurements, references, and other signals that are available for on-line control

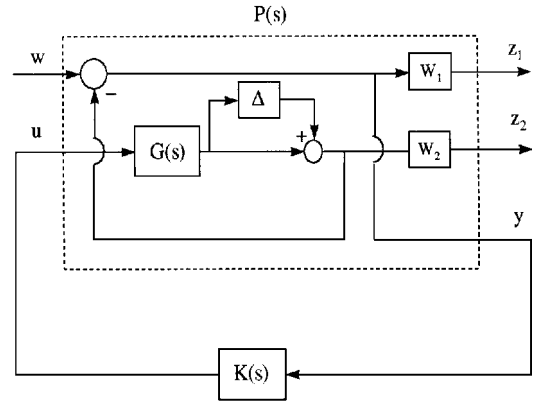

Fig. 3 Block diagram of weighted mixed-sensitivity objective function.

purposes. Signal $z = (z_1, z_2)$ is a vector whose elements comprise the cost functions given in Eq. (13).

Using linear fractional transformation theory,[27] these weighted cost functions are reformulated as

$$\boldsymbol{P}(s) = \begin{bmatrix} z_1 \\ z_2 \\ \boldsymbol{y} \end{bmatrix} = \begin{bmatrix} \boldsymbol{W}_1 & -\boldsymbol{W}_1\boldsymbol{G} \\ \boldsymbol{0} & \boldsymbol{W}_2\boldsymbol{G} \\ \boldsymbol{I} & -\boldsymbol{G} \end{bmatrix} \begin{bmatrix} \boldsymbol{w} \\ \boldsymbol{u} \end{bmatrix} \tag{14}$$

where $\boldsymbol{P}(s)$ is the generalized plant with realization $(\boldsymbol{A}_p, \boldsymbol{B}_p, \boldsymbol{C}_p, \boldsymbol{D}_p)$ and $\boldsymbol{K}(s)$ represents the $\mathcal{H}_\infty$ controller. The generalized plant is then described by a set of equations

$$\begin{gathered} \dot{\boldsymbol{x}} = \boldsymbol{A}_p\boldsymbol{x} + \boldsymbol{B}_{1p}\boldsymbol{w} + \boldsymbol{B}_{2p}\boldsymbol{u} \qquad z = \boldsymbol{C}_{1p}\boldsymbol{x} + \boldsymbol{D}_{11p}\boldsymbol{w} + \boldsymbol{D}_{12p}\boldsymbol{u} \\ \boldsymbol{y} = \boldsymbol{C}_{2p}\boldsymbol{x} + \boldsymbol{D}_{21p}\boldsymbol{w} + \boldsymbol{D}_{22p}\boldsymbol{u} \end{gathered} \tag{15}$$

where the system matrices are given by[28]

$$\boldsymbol{P}(s) = \left[\begin{array}{c|c} \boldsymbol{A}_p & \boldsymbol{B}_p \\ \hline \boldsymbol{C}_p & \boldsymbol{D}_p \end{array}\right] = \left[\begin{array}{ccc|cc} \boldsymbol{A} & \boldsymbol{0} & \boldsymbol{0} & \boldsymbol{0} & \boldsymbol{B} \\ \boldsymbol{B}_1\boldsymbol{C} & \boldsymbol{A}_1 & \boldsymbol{0} & \boldsymbol{B}_1 & -\boldsymbol{B}_1\boldsymbol{D} \\ \boldsymbol{B}_2\boldsymbol{C} & \boldsymbol{0} & \boldsymbol{A}_2 & \boldsymbol{0} & \boldsymbol{B}_2\boldsymbol{D} \\ \hline -\boldsymbol{D}_1\boldsymbol{C} & \boldsymbol{C}_1 & \boldsymbol{0} & \boldsymbol{D}_1 & -\boldsymbol{D}_1\boldsymbol{D} \\ \boldsymbol{D}_2\boldsymbol{C} & \boldsymbol{0} & \boldsymbol{C}_2 & \boldsymbol{0} & \boldsymbol{D}_2\boldsymbol{D} \\ -\boldsymbol{C} & \boldsymbol{0} & \boldsymbol{0} & \boldsymbol{I} & -\boldsymbol{D} \end{array}\right] \tag{16}$$

and where $\boldsymbol{x}(t) \in \mathcal{R}^n$, $\boldsymbol{w}(t) \in \mathcal{R}^{m_1}$, $\boldsymbol{z}(t) \in \mathcal{R}^{p_1}$, $\boldsymbol{u}(t) \in \mathcal{R}^{m_2}$, and $\boldsymbol{y}(t) \in \mathcal{R}^{p_2}$.

The $\mathcal{H}_\infty$ control algorithm used here is based on the one developed by Glover and Doyle (see Ref. 28). It is necessary to check for certain assumptions that are essential for applying the preceding algorithm. It is assumed that $(\boldsymbol{A}_p, \boldsymbol{B}_{2p})$ is stabilizable and $(\boldsymbol{C}_{2p}, \boldsymbol{A}_p)$ is detectable, which are necessary conditions for the existence of stabilizing controllers. To ensure realizability of the controller, it is assumed that the rank conditions $\operatorname{rank}(\boldsymbol{D}_{12p}) = \boldsymbol{m}_2$ and $\operatorname{rank}(\boldsymbol{D}_{21p}) = \boldsymbol{p}_2$ are satisfied. In addition, the rank conditions

$$\begin{gathered} \operatorname{rank}\begin{bmatrix} \boldsymbol{A}_p - j\omega\boldsymbol{I} & \boldsymbol{B}_{2p} \\ \boldsymbol{C}_{1p} & \boldsymbol{D}_{12p} \end{bmatrix} = n + m_2 \qquad \forall\omega \\ \operatorname{rank}\begin{bmatrix} \boldsymbol{A}_p - j\omega\boldsymbol{I} & \boldsymbol{B}_{1p} \\ \boldsymbol{C}_{2p} & \boldsymbol{D}_{21p} \end{bmatrix} = n + p_2 \qquad \forall\omega \end{gathered} \tag{17}$$

together with stabilizability and detectability conditions guarantee that the two Hamiltonian matrices have no eigenvalues on the imaginary axis. In the event that any of the rank conditions are violated, matrices $\boldsymbol{A}$ and/or $\boldsymbol{D}$ need to be modified[28] so that the behavior of the plant is changed very little over the significant range of frequencies.

Simulation Results

The parameters in Table 1 approximately represent those of the F-16 aircraft wing/store model with the GBU-8/B weapon system[19] and are used for the current simulation. Figure 4 shows the bending-

Table 1 Structural parameters

$m_s = 1027.6$ kg (2265 lb)	$x_\alpha = 0.178$ m (7.04 in.)
$m_w = 5.3\,m_s$	$x_\theta = 0$
$m_p = 1.361$ kg (3 lb)	$\ell = 0.223$ m (8.8 in.)
$r_\alpha = 0.635$ m (25 in.)	$L_1 = 0.223$ m (8.8 in.)
$r_\theta = 0.830$ m (32.7 in.)	$a = -0.152$
$b = 1.12$ m (44 in.)	$\omega_h = 24.5$ rad/s
$\omega_\theta/\omega_h = 0.55$	$\omega_\alpha/\omega_h = 1.27$

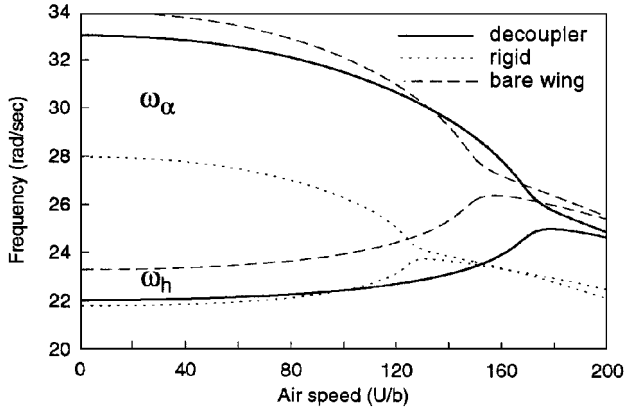

Fig. 4 Bending-torsion frequency coalescence vs air speed.

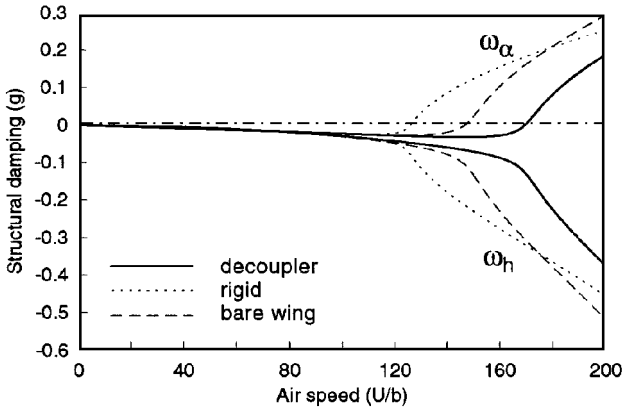

Fig. 5 Structural damping vs air speed.

torsion frequency coalescence trend as a function of air speed. The figure illustrates the effectiveness of the decoupler-pylon-mounted wing/store system over a rigidly mounted store in increasing the flutter speed. The frequencies at ground speed are those due to undamped, inertially coupled wing/store system, which are slightly reduced due to the apparent additional mass contributed by noncirculatory component of the aerodynamic loads [Eq. (6)]. As the flight speed is increased, the bending branch frequency for both the rigid and the decoupler cases remains approximately equal to its ground frequency, with a slight increase near the flutter speed. The first wing torsional mode frequency for the decoupler case, however, decreases relatively less than that corresponding to the rigid case because of the reduced store pitch inertia effects (due to the presence of soft-springlike actuator) and comes close to the bending branch near the flutter speed. The result is an increase in flutter speed for the decoupler-mounted store system. These branches do not coalesce because of the presence of aerodynamic damping present in the system.

The open-loop flutter speed, therefore, is predicted exactly from the V–g plot by calculating the speed where dissipation energy changes sign. The variation of bending and torsional mode structural damping as a function of air speed is shown in Fig. 5. It is observed that for both torsional and bending modes, the damping at first increases with air speed with the one corresponding to the bending branch increasing much rapidly than the torsional branch. At around 85–95% of the flutter speed, the torsional mode damping suddenly decreases and approaches zero at the flutter speed. The bending mode damping, however, continues to increase at a much faster rate. The open-loop flutter speed where the torsional mode damping changes sign is found to occur at $U/b = 170$ for decoupler case and $U/b = 127$ for rigid case. For comparison, the flutter speed for a clean wing (without any store) is found to be at $U/b = 148$. This represents a 14.86% increase in flutter speed with decoupler pylon over that of a bare wing and 33.86% increase over the rigidly attached case.

Therefore, the aim is to design an $\mathcal{H}_\infty$ controller that not only stabilizes the system at flutter speed but also maintains stability and nominal performance in the presence of the unstructured uncertainties discussed earlier. To design an $\mathcal{H}_\infty$ controller, appropriate weighting functions have to be first selected to be included in the generalized plant matrices [Eq. (16)]. The choice of weights is not trivial; weights are generally chosen purely as tuning functions to achieve the best compromise between conflicting objectives. However the selection is often guided by the need to reject unwanted signals such as errors, noises, etc., in a certain range of frequencies. Here the objective is to design a controller to achieve at least 10:1 reduction in the output errors (with respect to open-loop performance) in the presence of low-frequency (<30 rad/s) disturbances. This value of frequency is chosen so as to reject any unnecessary signals that are in the close range of critical flutter frequency ($\sim$25 rad/s). This frequency range also includes some typical disturbance frequencies such as those due to gusts ($\sim$6 rad/s), whose rejection is an important objective in the design process of a robust controller. For frequencies beyond 30 rad/s, a 40-dB/decade rolloff is desired, which places the control loop bandwidth at approximately 60 rad/s. Such a steep rolloff ensures that the controller is proper. A closed-loop bandwidth of 60 rad/s together with a second-order rolloff also ensures acceptable noise attenuation and sufficient stability margin to tolerate variations in the loop transfer matrix magnitude, which might arise due to unmodeled dynamics.

Based on the preceding design specifications, which quantify the tradeoff between nominal performance and robust stability, the following weighting matrices are constructed:

$$\boldsymbol{W}_1(s) = \gamma \frac{10(s/3674.2+1)^2}{(s/30+1)^2}\boldsymbol{I}_3 \tag{18}$$

$$\boldsymbol{W}_2(s) = \frac{(s+30)^2}{s+4500}\boldsymbol{I}_3 \tag{19}$$

A singular-value Bode plot of $\boldsymbol{W}_1^{-1}(s)$ and $\boldsymbol{W}_2^{-1}(s)$ depicting the design specifications for $\gamma = 1$ is shown in Fig. 6. The variable γ in $\boldsymbol{W}_1$ acts as a design parameter that is iteratively decreased until the norm in Eq. (13) is no longer satisfied. Physically, it gives relative importance to one of the two conflicting objectives of Eq. (13), without sacrificing compromise between them. The hinfopt routine in PRO-MATLAB's Robust Control Toolbox is used to find an optimum value of γ for the plant and given set of weighting functions, which after several iterations is found to be 0.0996. Therefore, the mathematically optimum performance (and, hence, robustness)

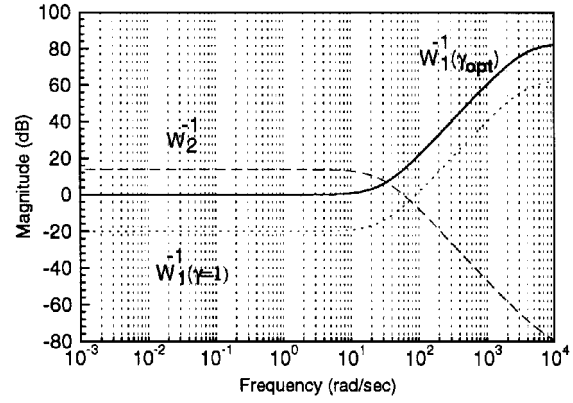

Fig. 6 Bode plot of W_1^{-1} and W_2^{-1}.

specification corresponding to $\gamma_{opt} = 0.0996$ has set the upper limit for achievable design without sacrificing the compromise between their objectives. The resulting deviation of the singular-value Bode plot of $\boldsymbol{W}_1^{-1}(s)$ for $\gamma_{opt} = 0.0996$ from its initial plot corresponding to $\gamma = 1$ is shown in Fig. 6.

Robust Stability and Nominal Performance Issues

A singular-value sufficiency test for stability robustness of a closed-loop system subjected to uncertainty due to unmodeled dynamics is obtained by applying the small gain theorem[26] to the loop in the block diagram of Fig. 3. For $\mathcal{H}_\infty$ problem formulation, all of the uncertainties discussed earlier are required to be reflected at the plant.[28] Application of the small gain theorem to the loop (Fig. 3) yields

$$\bar{\sigma}(\Delta)\bar{\sigma}\left(\frac{\boldsymbol{GK}}{\boldsymbol{I}+\boldsymbol{GK}}\right) < 1 \tag{20}$$

From Eq. (20), it is clear that the percentage tolerance bounds for output multiplicative perturbations can be obtained directly by looking at the singular-value plot of the complementary sensitivity function.

Figure 7 shows the closed-loop, singular-value Bode plot of the complementary transfer matrix $\boldsymbol{T}(j\omega)$ as a function of frequency ω. The absolute value of the maximum singular value of the $\boldsymbol{T}(j\omega)$ is found to be 16.42 dB, which implies that the closed-loop system is capable of withstanding at least $\pm 330\%$ plant uncertainty (with errors reflected at the output), without being destabilized. This magnitude of stability margin is observed to be at the flutter frequency (25 rad/s) where it is required to alleviate the effects of unmodeled dynamics, such as those due to wing/store aerodynamic and other flutter critical uncertainties. For frequencies beyond 25 rad/s, the percent tolerance bounds increase monotonically with the increase in frequency. Large endurance margins are necessary at such frequencies where the effects of ignoring aileron degree of freedom and other flexible modes including sensor and actuator dynamics are more prominent. Figure 7 also demonstrates that the compensated system has a nice noise attenuation property at the three outputs h, α, and θ, rejecting noise at high frequencies (>700 rad/s) by as much as 100 dB. On comparison with Fig. 6 [$\boldsymbol{W}_2^{-1}(s)$], it is clear that, whereas at higher frequencies the desired 40-dB/decade rolloff rate has been achieved, unnecessary noise attenuation is observed (for output h) at lower frequencies where its effect on the closed-loop response is typically negligible.

The characteristics of $\bar{\sigma}[\boldsymbol{S}(j\omega)]$ that are necessary for tracking step reference inputs and ensuring rejection of disturbances at the system output are shown in Fig. 8. The simulation shows that the disturbances entering at flutter frequency (25 rad/s) amplify the closed-loop response of the output θ with a magnitude of less than 0.27 dB. On the other hand, the same disturbances at the output h are rejected by 1.15 dB. This is to be expected as tradeoff between sensitivity and complementary sensitivity functions [$\boldsymbol{S}(s) + \boldsymbol{T}(s) = \boldsymbol{I}$] because from Fig. 7 it is indeed clear that outputs α and θ attenuate noise by a large magnitude, sometimes unnecessary at

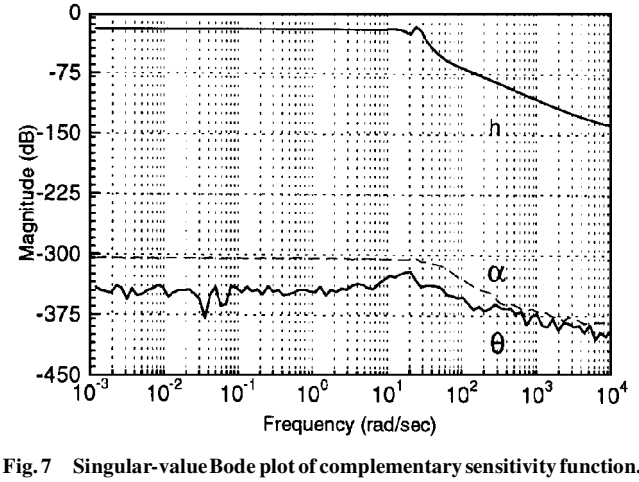

Fig. 7 Singular-value Bode plot of complementary sensitivity function.

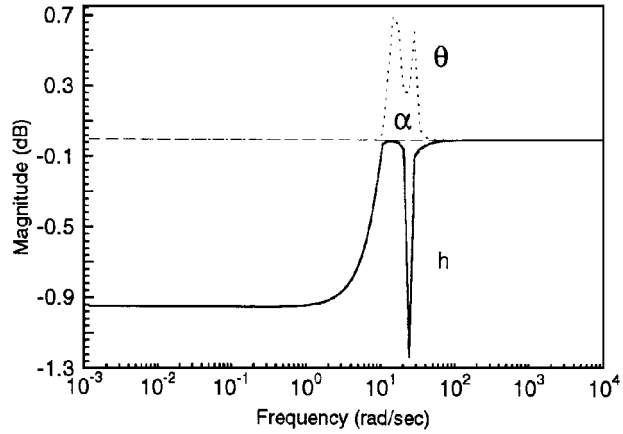

Fig. 8 Singular-value Bode plot of sensitivity function.

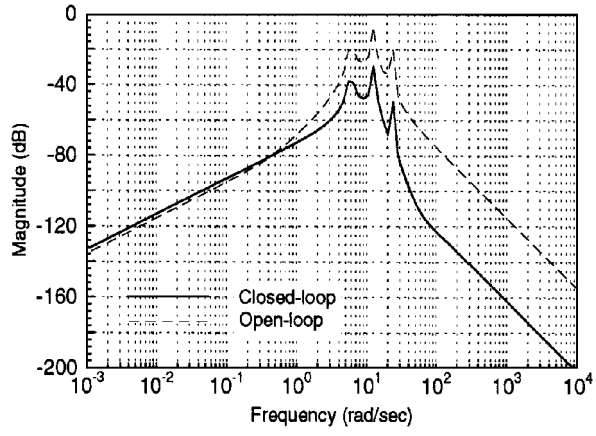

Fig. 9 Magnitude response from disturbance input to output.

frequencies where its effect is least likely to occur. This shows that perhaps by assigning unequal weights [as opposed to those given in Eq. (18)] to $\boldsymbol{W}_1^{-1}(s)$, with those corresponding to outputs α and θ weighed more strongly, better disturbance attenuation might have been achieved at those outputs. Nevertheless, for the low-frequency range (<10 rad/s), where the effect of gusts are more prominent, the plot shows that disturbances at outputs α and θ never get amplified if not rejected. This plot also gives the measure of relative insensitiveness to low-frequency wing/store parameter variations such as change in the c.g. location x_θ and radius of gyration r_θ of the store with flutter speed. A comparison of the open- and closed-loop magnitude response from disturbance input to output is shown in Fig. 9.

A sinusoidal input centered at 6 rad/s is used to model the disturbance. The singular-value Bode plot in Fig. 9 indicates that the closed-loop system has better rejection magnitude than the open-loop wing/store model. At very low frequencies less than 1 rad/s, the magnitude is almost the same for open- and closed-loop systems. For frequencies beyond 1 rad/s and particularly at flutter frequency (25 rad/s), the closed-loop system rejects disturbances by as much as 25 dB more than that of the open-loop system.

Finally, the singular-value Bode plot of the controller (Fig. 10) approximately shows the characteristics of a first-order system with a break frequency of 20 rad/s. A 17-state strictly proper controller is obtained by solving the four-block mixed-sensitivity $\mathcal{H}_\infty$ problem. The controller has a large gain of 50 dB for frequencies less than 5 rad/s and a bandwidth of 500 rad/s (as shown in Fig. 10). These properties are required to be able to withstand sudden (additive) perturbations in the outputs of the plant. But, in most applications, a controller with limited bandwidth is desired to prevent pushing the actuators beyond their limits and to avoid the controller exciting high-frequency discarded modes. It also facilitates digital implementation wherein issues of sampling frequencies need to be further taken care of.

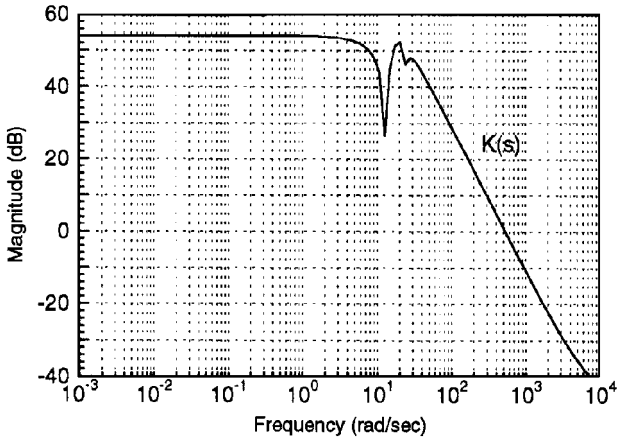

Fig. 10 Bode plot of $\mathcal{H}_\infty$ controller transfer function.

Conclusions

An active decoupler pylon concept is presented for the wing/store flutter suppression problem. A mixed-sensitivity minimization problem is solved to design a $\mathcal{H}_\infty$ controller, and its effectiveness in addressing the robust stability and nominal performance issues pertaining to the store flutter problem is studied. The simulation results indicate sufficient tolerance margins to unstructured uncertainties arising at high-frequency ranges due to discarded dynamics. In particular, the margin at the flutter frequency appears to be satisfactory where the effect on flutter speed is more prominent due to neglected store aerodynamics and fuselage dynamics. Nice sensitivity properties are obtained at the outputs, although they have been underachieved in a certain range of frequencies. In particular, around the flutter frequency, the relative angle between the wing and the store shows sensitiveness to external output disturbances and low-frequency parameter variations. Although its sensitivity magnitude is not that large, it may pose a potential problem to the actuator's performance. Noise attenuation properties at the three outputs show overachievement of the objective at all of the frequencies. By appropriately emphasizing the frequency-dependent weighting functions for each of the outputs, the problem of over- and underachievement of the objectives can perhaps be addressed. The control law shows favorable large gain and bandwidth typically required to withstand sudden variations at plant output. Comparison with open-loop response shows that the closed-loop system is able to withstand and reject low-frequency disturbances and parameter variations. Overall, the $\mathcal{H}_\infty$ design technique has been successful in giving the control engineer relative freedom to address the tradeoff between robust stability and nominal performance issues related to the wing/store flutter problem.

Acknowledgments

The authors are grateful for the generous support of the Air Force Office of Scientific Research (AFOSR-F49620-95-1-0362) under the direction of Capt. Brian Sanders.

References

[1]Mykytow, W. J., "Recent Analysis Methods for Wing/Store Flutter," *Specialist Meeting on Wing-With-Stores Flutter*, AGARD-CP-162, April 1962.

[2]Katz, H., "Flutter of Aircraft with External Stores," *Proceedings of Aircraft Stores Symposium*, Vol. 2, U.S. Air Force Armament Development and Test Center, Eglin AFB, FL, Nov. 1969.

[3]Foughner, J. T., Jr., and Besinger, C. T., "F-16 Flutter Model Studies of External Wing Stores," NASA-TM-74078, Oct. 1977.

[4]Triplett, W. E., "A Feasibility Study of Active Wing/Store Flutter Control," *Journal of Aircraft*, Vol. 9, No. 6, 1972, pp. 438–444.

[5]Noll, T. E., Felt, L. R., Mykytow, W. J., and Russell, H. L., "Potential Application of Active Flutter Suppression to Future Fighter Attack Aircraft," *Aircraft/Stores Compatibility Symposium Proceedings*, Vol. 5, 1973, pp. 18–20.

[6]Sandford, M. C., Abel, I., and Gray, D. L., "Development and Demonstration of a Flutter Suppression System Using Active Controls," NASA-TR-R-450, Dec. 1975.

[7]Harvey, C. T., Johnson, T. L., and Stein, G., "Adaptive Control of Wing/Store Flutter," U.S. Air Force Flight Dynamics Lab., AFFDL-TR-79-3081, Wright–Patterson AFB, OH, April 1979.

[8]Haidl, G., Lotze, A., and Sensburg, O., "Active Flutter Suppression on Wings with External Stores," AGARD-AG-175, 1974, pp. 57–74.

[9]Hönlinger, H., "Active Flutter Suppression on an Airplane with Wing Mounted External Stores," AGARD-CP-228, Aug. 1977.

[10]Hönlinger, H., and Destuynder, R., "External Store Flutter Suppression with Active Controls," *Lecture Series*, von Kármán Inst. for Fluid Dynamics, Vol. 2, Dec. 1978, pp. 1–85.

[11]Reed, W. H., III, Foughner, J. T., Jr., and Runyan, H. L., "Decoupler Pylon: A Simple Effective Wing/Store Flutter Suppressor," *Journal of Aircraft*, Vol. 17, No. 3, 1980, pp. 206–211.

[12]Triplett, W. E., Kappus, H. P. F., and Landy, R. J., "Active Flutter Suppression Systems for Military Aircraft—A Feasibility Study," U.S. Air Force Flight Dynamics Lab., AFFDL-TR-72-116, Wright–Patterson AFB, OH, Feb. 1973.

[13]Runyan, H. L., "Effect of a Flexibly Mounted Store on the Flutter Speed of a Wing," NASA-CR-159245, April 1980.

[14]Desmarais, R. N., and Reed, W. H., III, "Wing/Store Flutter with Nonlinear Pylon Stiffness," *Journal of Aircraft*, Vol. 18, No. 11, 1981, pp. 984–987.

[15]Lottati, I., "Aeroelastic Tailoring of a Composite Wing with a Decoupler Pylon as a Wing/Store Flutter Suppressor," *Journal of Aircraft*, Vol. 25, No. 3, 1988, pp. 271–280.

[16]Yang, Z.-C., and Zhao, L.-C., "Wing-Store Flutter Analysis of an Airfoil in Incompressible Flow," *Journal of Aircraft*, Vol. 26, No. 6, 1989, pp. 583–587.

[17]Yang, Y.-R., "KBM Method of Analyzing Limit Cycle Flutter of a Wing with an External Store and Comparison with a Wind-Tunnel Test," *Journal of Sound and Vibration*, Vol. 187, No. 2, 1995, pp. 271–280.

[18]Peloubet, R. P., Jr., Haller, R. L., and McQuien, L. J., "Feasibility Study and Conceptual Design for Application of NASA Decoupler Pylon to the F-16," NASA-CR-165834, May 1982.

[19]Clayton, J. D., Haller, R. L., and Hassler, J. M., Jr., "Design and Fabrication of the NASA Decoupler Pylon for the F-16 Aircraft," NASA-CR-172354, Jan. 1985.

[20]Gade, P. V. N., and Flowers, G. T., "Flutter Suppression of an Airfoil with Unsteady Forces Using a Piezoelectric Active Strut," AIAA Paper 94-1746, April 1994.

[21]Pokines, B., Belvin, W. K., and Inman, D. J., "Static and Dynamic Characteristics of a Piezoceramic Strut," *Proceedings of the AIAA/DOD 5th Control-Structures Interaction Technology Conference*, 1992, pp. 133–140.

[22]Theodorsen, T., "General Theory of Aerodynamic Instability and the Mechanism of Flutter," NACA Rept. 496, May 1935, pp. 413–433.

[23]Edwards, J. W., "Unsteady Aerodynamic Modeling and Active Aeroelastic Control," Stanford Univ., Rept. SUDAAR 504, Stanford, CA, Feb. 1977.

[24]Jones, R. T., "Operational Treatment of the Nonuniform Lift Theory to Airplane Dynamics," NACA TN 667, March 1938, pp. 347–350.

[25]Zhou, K., Doyle, J. C., and Glover, K., *Robust and Optimal Control*, Prentice–Hall, Englewood Cliffs, NJ, 1996, Chap. 9.

[26]Dailey, R. L., *Lecture Notes for the Workshop on $\mathcal{H}_\infty$ and μ Methods for Robust Control*, American Control Conf., 1990, pp. 1–116.

[27]Green, M., and Limebeer, D. J. N., *Linear Robust Control*, Prentice–Hall, Englewood Cliffs, NJ, 1995, Chap. 4.

[28]Maciejowski, J. M., *Multivariable Feedback Design*, Addison–Wesley, Wokingham, England, UK, 1993, Chap. 6.